Oxygen Gas Abundances at $z \sim 1.4$: Implications for the Chemical Evolution History of Galaxies[0]

C. Maier[1]

chmaier@phys.ethz.ch

S.J. Lilly[1], C. M. Carollo[1], K. Meisenheimer[2], H. Hippelein[2], and A. Stockton[3]

ABSTRACT

The $1 < z < 2$ redshift window hosts the peak of the star formation and metal production rates. Studies of the metal content of the star forming galaxies at these epochs are however sparse. We report VLT-ISAAC near-infrared spectroscopy for a sample of five [OII]-selected, $M_{B,AB} \lesssim -21.5$, $z \sim 1.4$ galaxies, by which we measured Hβ and [O III] λ 5007 emission line fluxes from J-band spectra, and Hα line fluxes plus upper limits for [N II] λ 6584 fluxes from H-band spectra. The $z \sim 1.4$ galaxies are characterized by the high [OIII]/[OII] line ratios, low extinction and low metallicity that are typical of lower luminosity CADIS galaxies at $0.4 < z < 0.7$, and of more luminous Lyman Break Galaxies at $z \sim 3$, but not seen in CFRS galaxies at $0.4 \lesssim z \lesssim 0.9$. This type of spectrum (e.g., high [O III] λ 5007/[O II] λ 3727) is seen in progressively more luminous galaxies as the redshift increases. These spectra are caused by a combination of high ionisation parameter q and lower [O/H]. Pégase2 chemical evolution models are used to relate the observed metallicities and luminosities of $z \sim 1.4$ galaxies to galaxy samples at lower and higher redshift. Not surpringsingly, we see a relationship between redshift and inferred chemical age. We suppose that the metal-enriched reservoirs of star forming gas that we are probing at intermediate redshifts are being mostly consumed to build up both the disk and the bulge components of spiral galaxies. Finally, our analysis of the metallicity-luminosity relation at $0 \lesssim z \lesssim 1.5$ suggests that the period of rapid chemical evolution may take place

[0]Based on observations obtained at the ESO VLT, Paranal, Chile; ESO program 074.B-0122

[1]Department of Physics, Swiss Federal Institute of Technology (ETH Zürich), ETH Hönggerberg, CH-8093, Zürich, Switzerland

[2]Max–Planck–Institut für Astronomie, Königstuhl 17, D-69117 Heidelberg, Germany

[3]Institute for Astronomy, University of Hawaii, 2680 Woodlawn Drive, Honolulu, HI 96822

progressively in lower mass systems as the universe ages. These results are consistent with a "downsizing" type picture in the sense that particular signatures (e.g., high [OIII]/[OII] or low [O/H]) are seen in progressively more luminous (massive) systems at higher redshifts.

Subject headings: galaxies: abundances, galaxies: evolution, galaxies: high redshift

1. Introduction

Gas metallicities are a particularly important diagnostic of galaxy evolution: at any given epoch, in any given galaxy population, they trace the amount of metals which have been produced and assembled by its previous stellar generations, as well as the metals which will be locked in its future generations of stars.

Efforts to determine the gas metallicity of star forming galaxies as a function of cosmic time have returned oxygen ([O/H]) gas metallicities for relatively large sample of galaxies up to $z \sim 1$ and a handful above $z \sim 2$ (Carollo and Lilly 2001, hereafter Paper I; Lilly et al. 2003, hereafter Paper II; Kobulnicky et al. 2003; Maier et al. 2004; Pettini et al. 2002; Maier et al. 2005, hereafter Paper III). Most of these studies have relied on rest-frame optical lines, and in particular on the $R_{23} = ([\mathrm{O\,II}]\,\lambda\,3727 + [\mathrm{O\,III}]\,\lambda\lambda\,4959, 5007)/\mathrm{H}\beta$ metallicity indicator (Pagel et al. 1979). While relatively easy to measure, R_{23} is however degenerate with metallicity (as low values of R_{23} may correspond to very low or high metallicities), and affected by dust extinction. Both problems are solved if the Hα and $[\mathrm{N\,II}]\,\lambda\,6584$ line fluxes are also available, since the Hα/Hβ line ratio provides an estimate for the dust extinction, and the $[\mathrm{N\,II}]\,\lambda\,6584$/H$\alpha$ line ratio breaks the degeneracy in R_{23}.

The reason for which most quoted studies have not used the Hα and $[\mathrm{N\,II}]\,\lambda\,6584$ lines is a practical one. For $z \gtrsim 0.5$ these two lines are shifted in the near-infrared (NIR), and are thus much more challenging to measure than the lines which appear within the optical window. Nonetheless, these two lines turn out to be important to the study of galaxy properties at high-z. In Paper III we used VLT-ISAAC and Keck-NIRSPEC NIR spectroscopy to measure Hα and $[\mathrm{N\,II}]\,\lambda\,6584$ emission line fluxes – and thus individual extinction values and reliable metallicities – for 30 $0.47 < z < 0.92$ galaxies extracted from the Canada France Redshift Survey (Lilly et al. 1995a, CFRS). We measured a large ~ 3 mag scatter in extinction values for the CFRS galaxies, which demonstrated the importance of individual extinction corrections in order to avoid errors in the determination of star forming rates and metallicities of high z galaxies.

The next step is to extend a similar study of the star forming gas metallicity to galaxies at higher redshifts. The rather unexplored $1 < z < 2$ redshift regime is one of particular importance in the history of the universe: there, the star formation and metal production rates for the universe as a whole, as measured by the the integrated luminosity density in the ultraviolet and far-infrared, appear to peak, i.e., are a factor of about 6 higher relative to the local value (see, e.g., Lilly et al. 1996; Madau et al. 1996; Chary & Elbaz 2001; Somerville et al. 2001; Perez-Gonzalez et al. 2005). Furthermore, this is the redshift regime where the galaxy population clearly undergoes a transition in properties: it is beyond $z \sim 1$ that luminous ultraviolet star-forming galaxies with "unobscured" star-formation rates (SFRs) $\dot{M} > 10$ $M_{\odot}yr^{-1}$, e.g., galaxies with $L_{[OII]3727} > 10^{42}$ erg s^{-1} (Cowie et al. 1995), appear in optically-selected galaxy samples. Such galaxies are not detected below $z \sim 0.8 - 1.0$ (see, e.g., Cowie et al. 1995).

Due to the paucity in observable windows of spectral diagnostics for galaxies in the $1 < z < 2$ redshift range, the gas metallicities (and more generally the physical properties) of $1 < z < 2$ galaxies are still mostly unconstrained. Luckily, for the specific redshift $z \sim 1.4$, all five emission lines which are key to determine the gas metallicity and the extinction, i.e., [O II] λ 3727, Hβ, [O III] λ 5007, Hα, and [NII], are all observable within several (near-infrared) atmospheric windows (there is also another such window at $z \sim 2.3$). At the extreme redshift limit of ground-based optical surveys [O II] λ 3727 can be detected up to $z \sim 1.5$ in the 9200 Å atmospheric window, e.g. in the CFRS survey. Furthermore, other surveys have exploited explicitly the 9200 Å atmospheric window: the CADIS survey (see e.g., Maier 2002) and other searches for $z \sim 6.6$ Lyman α emitters (Crampton & Lilly 1999; Tran et al. 2004) have produced, as foreground interlopers, several [O II] λ 3727-selected $z \sim 1.4$ galaxies. The $z \sim 1.4$ epoch lies roughly midway in cosmic time between the $0.5 < z < 1.0$ redshift range probed, e.g., by the CADIS (Maier et al. 2004) and CFRS galaxies (Paper III), and the $z \sim 3$ epoch characterized by the LBGs (for a handful of which oxygen abundances have been measured by Pettini et al. 2001).

In this paper we present oxygen gas abundances for a sample of five galaxies at $z \sim 1.4$ selected by their [O II] λ 3727 emission. The paper is structured as follows: In Sect. 2 we describe the VLT-ISAAC observations of our sample galaxies, and present the lower redshift samples that we use for comparison in our discussion. In Sect. 3 we present the derived emission line fluxes, metallicities and extinction values derived (as in Paper III) using a representation of the Kewley & Dopita (2002, hereafter KD02) models. In Sect. 4 we present a grid of Pégase2 chemical evolution models, and discuss those which are compatible with the observations. We then compare our metallicity measurements at $z \sim 1.4$ with similar measurements at other redshifts, and with the Pégase2 models, and discuss the picture for the chemical evolution of galaxies that emerges from our study. Finally, in Sect. 5 we

present our conclusions. A *concordance*-cosmology with $H_0 = 70$ km s^{-1} Mpc^{-1}, $\Omega_0 = 0.3$, $\Omega_\Lambda = 0.7$ is used throughout this paper. Our measurements of [O/H] do not depend on the solar [O/H]. However, when linking the oxygen abundance with the metallicity calculated in Pégase2 models we use the solar value $12 + \log(\mathrm{O/H}) = 8.87$ from Grevesse et al. (1996). Note that *metallicity* and *abundance* will be taken to denote *oxygen abundance* throughout this paper, unless otherwise specified.

2. The data

2.1. Sample, observations and data reduction

The sample galaxies were selected as [O II] λ 3727 - emitters at $z \sim 1.4$ from three sources: the CADIS survey (see, e.g., Maier 2002; Maier et al. 2003), the CFRS survey (Lilly et al. 1995b), and from unpublished analysis of CFHT emission line searches in the CFRS 22h field (Crampton & Lilly 1999; Tran et al. 2004). The [O II] λ 3727 lines of the CADIS galaxies were measured using a Fabry-Perot interferometer at about 9200Å (for details, see Hippelein et al. 2003; Maier et al. 2003). The CFHT survey was undertaken combining multiple parallel long slits with a narrowband filter to search for $z \sim 6.6$ Lyman α emitters in the 9200 Å atmospheric window (for details see Crampton & Lilly 1999; Tran et al. 2004). These CFHT [O II] λ 3727 -selected galaxies are located in the CFRS 22h field (Lilly et al. 1995b).

The total sample of $z \sim 1.4$ galaxies contains five objects, two from the CADIS, one from the CFRS survey, and two from the CFHT multislit+narrowband filter survey. For all galaxies we obtained VLT-ISAAC spectra in the J band, to measure the Hβ and [O III] λ 5007 fluxes, and in the H-band, to measure Hα and (upper limits to the) [NII] fluxes. We also acquired H- and J-band imaging in order to test the relative calibration of the emission line fluxes, as described in Paper III. Fragmentary near-infrared spectroscopy data were obtained for three additional objects, and we will report these elsewhere if we made up the remaining flux measurements.

The observations were carried out at the VLT in visitor mode in October 2004 (Program 074.B-0122A) using a slit of 2″ width and 120″ length. The spectra cover a range of 79 nm in the H band, and 59 nm in the J band. The individual integration times and the standard stars used for the flux calibration are given in Table 1. The data reduction was done using IRAF as described in detail in Paper III for similar ISAAC spectroscopic observations of CFRS galaxies at medium redshift. The resulting spectra of the five $z \sim 1.4$ galaxies are shown in Figure 1. For easy reference we use throughout this paper the galaxy

identification codes adopted in the previous quoted literature.

In the good seeing conditions for the ISAAC observations (see Table 1), the 2″ ISAAC slit approximates a total flux measurement. It is well matched to the 1″.75 width of the CFRS observations for CFRS-221153 (Le Fevre et al. 1995) and to the 2″ width of the slit used for the observations of LTBC-18A and LTBC-18B (Crampton & Lilly 1999; Tran et al. 2004). The [O II] λ 3727 measurements for the two CADIS objects were made with an imaging Fabry-Perot interferometer (see, e.g., Maier et al. 2003) and thus the measured flux should be "total". In Paper III we were able to check directly the relative flux calibration of optical and near-infrared spectra, under similar observational set-ups, and concluded that there was no evidence of problems. One possible concern with the present data is that the slits used by Crampton & Lilly (1999) may not have been accurately centered on the two LTBC objects, conceivably leading to an underestimate of the [O II] λ 3727 flux for these particular objects. However, these two objects have similar emission line ratios to the other $z \sim 1.4$ galaxies and slit mis-centering is not believed to be a problem.

2.2. Comparison samples

In this paper we compare our new $z \sim 1.4$ metallicities data with the properties of 30 CFRS galaxies at $0.47 < z < 0.92$ from Paper III, and with 17 lower luminous $0.4 < z < 0.7$ CADIS galaxies from Maier et al. (2004). Although only few of the $0.4 < z < 0.7$ CADIS galaxies have five emission lines observed, Maier et al. (2004) showed that it is likely that all 17 CADIS galaxies have low extinction, so we used the case B intensity ratio of Hα to Hβ of 2.86 when running our program to determine metallicities based on the KD02 models. As nearby comparison samples we adopted, as in Paper III, 70 $z < 0.095$ KISS galaxies of Melbourne & Salzer (2002), and 108 NFGS $z < 0.04$ galaxies of Jansen et al. (2000), with all [O II] λ 3727, Hβ, [O III] λ 5007, Hα, and [NII] line fluxes measured.

After careful analysis, we opted for *not* using, in our analysis of the metallicities, the following samples of galaxies with published oxygen metallicities: the 64 $0.26 < z < 0.82$ galaxies of Kobulnicky et al. (2003), the 177 $0.3 < z < 1$ galaxies of Kobulnicky & Kewley (2004), the 25 $0.4 < z < 0.9$ galaxies of Liang et al. (2004), and the 7 galaxies at $2.1 < z < 2.5$ of Shapley et al. (2004). In fact, from all these samples, only a handful of low redshift (typically $z \lesssim 0.5$) objects had Hα and [N II] λ 6584 measurements, which are important to break the R_{23} degeneracy with metallicity. In detail, 9/66 galaxies at $0.26 < z < 0.82$ with measured equivalent widths from Kobulnicky et al. (2003) have measured [N II] λ 6584/Hα (all at $z < 0.4$); 32/177 galaxies at $0.3 < z < 1$ with measured equivalent widths from Kobulnicky & Kewley (2004) have measured [N II] λ 6584/Hα (all at $z < 0.5$);

and 4/25 galaxies at $0.4 < z < 0.9$ from Liang et al. (2004) have [N II] λ 6584/Hα measured. Furthermore, several of the mentioned studies performed no dust extinction correction. This, as we showed in Paper III, can significantly affect the analysis. Finally, the $2.1 < z < 2.5$ galaxies of Shapley et al. (2004) had oxygen abundances determined using only the [N II] λ 6584/Hα ratio; these, as already discussed by Shapley et al. (2004) and in Paper III, are on their own rather uncertain (see also van Dokkum et al. 2005). We do not think that excluding these samples from our discussion would significantly change our conclusions. Moreover, as discussed below, using the CADIS and CFRS comparison samples has several advantages.

2.2.1. Advantages of the CADIS and CFRS comparison samples

The choice of the CADIS and CFRS samples for comparison with our new set of metallicities for galaxies at $z \sim 1.4$ has two main advantages:

i) As stressed by Salzer et al. (2005), the details of any specific calibration of line fluxes and ratios into metallicity has a significant impact on the metallicity measurements and the resulting luminosity-metallicity relation. It is thus important that, when comparing different samples of galaxies, identical methods and calibrations are adopted for all samples (see also Ellison & Kewley 2005). For all the galaxies of the adopted comparison samples we had access to the emission line fluxes measurements and derived [O/H] metallicities using the same approach that we used for calculating the metallicities of the $z \sim 1.4$ galaxies (see Section 3.2, and Paper III for details on the method).

ii) Another important requirement for performing a proper comparison of the metallicity-luminosity relation between low- and high-z samples of galaxies is the availability of properly derived rest-frame luminosities for the distant galaxies. As also stressed by Salzer et al. (2005), one should fit the full SEDs over a large wavelength range in order to obtain reliable rest-frame luminosities for the $z > 0$ galaxies. We have available multi-wavelength imaging for the $z \sim 1.4$ galaxies presented in this paper, as well as for the CFRS galaxies of Paper III (see Table 1 of Paper III), and the CADIS objects where 16 filters were used to derive the SED (see Hippelein et al. 2003; Maier et al. 2004). Reliable rest-frame luminosities could therefore be obtained for all the galaxies in these samples.

2.2.2. Selection effects in the CADIS and CFRS samples

The CADIS and CFRS galaxies at $0.4 < z < 1$ have different selection criteria, but, excluding a few objects, we can get a useful comparison sample, as shown in the following. The CFRS galaxies are selected to have $I_{AB} < 22.5$, and a rest frame equivalent width of Hβ, EW_0(Hβ), larger than 8 Å, as described in Paper II. On the other hand, the CADIS galaxies were selected based on their [O III] λ 5007 emission detected using a Fabry-Perot-Interferometer ($F_{\rm lim} = 3 \cdot 10^{-20}$Wm^{-2}), regardless of their continuum brightness. Thus, CADIS can detect lower luminosity galaxies at a given z.

Fig. 2 shows the distribution of EWs at restframe wavelength of $z \sim 1.4$, CADIS and CFRS galaxies as a function of blue absolute magnitude. The distribution of EWs of the CADIS galaxies is broadly consistent with the EW distribution of CFRS and $z \sim 1.4$ galaxies (and this holds also for the larger CADIS sample as shown in Fig. 4 in Hippelein et al. 2003), except for three CADIS objects at $z \sim 0.4$ (open circles) which have a particular high EW. These are the only galaxies without VLT spectroscopic follow-up reported by Maier et al. (2004), galaxies with high enough fluxes that their oxygen abundance could be obtained using spectroscopy with the 3.6-m Telescopio Nazionale Galileo (TNG). We will exclude these three objects from the CADIS comparison sample in the following.

Summarizing the above, despite the different selection criteria, the $M_{B,AB} < -21.5$ $z \sim 1.4$ galaxies, the $M_{B,AB} < -19.5$ CFRS, and the $-17.5 > M_{B,AB} > -19.5$ CADIS sample follow a similar EW-$M_{B,AB}$ distribution (after excluding the three objects mentioned above) suggesting that they are not completely different species and that the CADIS+CFRS sample is a useful comparison sample for the $z \sim 1.4$ galaxies. It is not perfect, but it is the best we can do at the present time. The CADIS objects were [OIII] selected, whereas the CFRS is effectively Hβ selected (see Paper II). It should be appreciated that CADIS will be slightly biased towards high [OIII]/[OII] (and low [O/H]), inferred from the fact that there is a correlation within the CFRS sample between $L_{[OIII]}$ and [OIII]/[OII], and $L_{[OIII]}$ and [O/H]. There is no such correlation with $L_{[OII]}$, indicating that there should not be similar biases in the $z \sim 1.4$ [O II] λ 3727 selected sample.

3. The measurements

3.1. Emission line fluxes

Emission line fluxes were measured from the calibrated spectra following the procedure described in Paper III. Table 2 reports, for each individual galaxy, the emission line fluxes

(or upper limits) of the five observed galaxies. Specifically:

(i) The [N II] λ 6584 line was too faint to be detected. However, we could determine upper limits to the [N II] λ 6584 flux for all five $z \sim 1.4$ galaxies, which are good enough to check for contamination by AGNs and to break the degeneracy of the R_{23} relation. Table 2 lists the 2σ upper limits.

(ii) For four of the $z \sim 1.4$ galaxies we were able to measure fluxes for all three lines of Hβ, [O III] λ 5007, and Hα. The fluxes and flux errors were measured as described in Paper III. We have not applied any corection for stellar absorption to the Hβ line, because this line has an observed equivalent width larger than 50Å for the four $z \sim 1.4$ galaxies. Like in Paper III, we assumed a minimum 10% for the uncertainties of the measured fluxes when computing oxygen abundances using the KD02 models (see Table 2).

(iii) For the galaxy CADIS-01h-11134 the Hβ line coincides with a strong OH line, so we were not able to measure the Hβ line flux. However, we could measure [O II] λ 3727, [O III] λ 5007, Hα, and an upper limit for [N II] λ 6584 for this galaxy. We calculated the Hβ flux for the galaxy CADIS-01h11134 using case B recombination and assuming a low $A_V = 0.5$ (similar to the extinction values found for the other four $z \sim 1.4$ galaxies), and we used this value when calculating the oxygen abundance of this galaxy using the models of KD02 (see Section 3.2). This results in a value of $A_V = 0.39^{+0.43}_{-0.39}$, which is completely consistent with the input value. This makes the point that A_V is not solely determined by Hα/Hβ, but also has a small contribution from the other line ratios.

3.2. Gas metallicities, SFRs and extinction parameters

The approach described in Paper III was used to derive [O/H] and the extinction values A_V for the five $z \sim 1.4$ galaxies. Briefly, the approach is based on the models of KD02, who developed a set of ionisation parameter and oxygen abundance diagnostics based on the use of strong rest-frame optical emission lines. The method consists in performing a simultaneous fit to all available emission line fluxes (including the [N II] λ 6584 upper limits) in terms of extinction parameter A_V, ionisation parameter q, and [O/H].

As in Paper III, before proceeding with determining gas metallicities, we checked that the detected line emission is not strongly contaminated by the presence of an AGN. To this purpose we used the log([O III] λ 5007/Hβ) vs. log([N II] λ 6584/Hα) diagnostic diagram shown in Fig. 3. The location on this diagram of the five $z \sim 1.4$ galaxies is indicated with arrows, given that we only had upper limits for the [NII] fluxes. The five galaxies lie under and to the left of the theoretical curve of Kewley et al. (2001, solid line), which separates

star forming galaxies (below/left of the curve) from AGNs (above/right of the curve). In none of the five $z \sim 1.4$ galaxies the line emission is therefore dominated by an AGN.

The gas metallicities we then derived for the $z \sim 1.4$ galaxies are rather low compared to lower redshift galaxies of similar luminosities, and also their derived extinction values are quite low. We will discuss this finding in the following Sect. 4. The Hα luminosities (corrected for extinction) were used to calculate the SFRs of the five $z \sim 1.4$ galaxies using the Kennicutt (1998) conversion of Hα luminosity into $\dot{\rm M}$: SFR($\rm M_\odot yr^{-1}$) = 7.9×10^{-42}L(Hα)ergs/s. The resulting SFRs are given in Table 2. Note that alternative (but less probable) oxygen abundance solutions are found for two $z \sim 1.4$ galaxies, and we will indicate them as open squares wherever [O/H] is plotted. These alternative (but less probable) oxygen abundances found using the method described in Section 3.3 of Paper III are [O/H]=$8.02^{+0.10}_{-0.07}$ for object LTBC-18A, and [O/H]=$8.34^{+0.16}_{-0.12}$ for object CADIS-23h-3487.

4. Discussion

4.1. Basic observational result

Our basic observational result is that the spectra of the $z \sim 1.4$ galaxies, which have $-21.5 \gtrsim M_{B,AB} \gtrsim -23$ have the line ratios and derived parameters (metallicity, extinction, ionisation parameter) that are found in much lower luminosity galaxies at lower redshifts. Specifically, they are similar to what is found in the $0.4 < z < 0.7$ CADIS galaxies ($M_{B,AB} > -19.5$), and noticably different from the general properties of the more luminous ($-19.5 > M_{B,AB} > -22$) CFRS galaxies at $0.47 < z < 0.92$ (see Paper III).

We look first at the simple line ratios. Fig. 4 shows the location of the five $z \sim 1.4$ galaxies on the diagnostic diagram [O III] λ 5007/[O II] λ 3727 (extinction corrected) vs. [O III] λ 5007/Hβ. The lower luminosity $0.4 < z < 0.7$ CADIS galaxies, the brighter $0.47 < z < 0.92$ CFRS galaxies, and the more luminous $z \sim 3$ LBGs are also plotted for comparison. In contrast with the bright, intermediate-z CFRS galaxies, which show low [O III] λ 5007/[O II] λ 3727 and [O III] λ 5007/Hβ ratios, it should be noted that all the $z \sim 1.4$ galaxies have the high [O III] λ 5007/[O II] λ 3727 and [O III] λ 5007/Hβ line ratios which are typical of the lower luminosity intermediate-z CADIS galaxies and of the more luminous LBGs at higher z. In other words, the appearance of high [O III] λ 5007/[O II] λ 3727 ratios moves to brighter luminosities at higher z.

To illustrate this further, Fig. 5 shows the line ratios [O III] λ 5007/[O II] λ 3727 vs. $M_{B,AB}$ for the five $z \sim 1.4$ galaxies, the CADIS and CFRS sample, the LBGs, and the local KISS and NFGS galaxies. It is clear that there is a relation between [O III] λ 5007/[O II] λ 3727

and $M_{B,AB}$ for local KISS galaxies, in the sense that lower luminosity galaxies tend to have higher [O III] λ 5007/[O II] λ 3727 ratios. At higher redshifts, a similar trend is seen for the combined sample of CADIS and CFRS galaxies at $0.4 \lesssim z \lesssim 0.9$, with the relation displaced upwards and to the right, i.e. to higher [O III] λ 5007/[O II] λ 3727 ratios at a given luminosity or higher luminosities at a given line ratio. The $z \sim 1.4$ and LBG galaxies at $z \sim 3$ continue this trend, uniformly exhibiting the high [O III] λ 5007/[O II] λ 3727 ratios (i.e. above one). While the [O III] λ 5007/[O II] λ 3727 distribution of the [O III] λ 5007 selected CADIS objects may be biased (see Section 2.2.2), the $z \sim 1.4$ galaxies were [O II] λ 3727-selected and there is no observational selection against low [O III] λ 5007/[O II] λ 3727 ratios.

The tracks of individual galaxies in this diagram are likely to be diagonal, moving down to lower [O III] λ 5007/[O II] λ 3727 with modest fading. Within the population, the evolutionary trend is in the sense that, as we look back in time, galaxies of similar luminosities as local galaxies show increasingly higher [O III] λ 5007/[O II] λ 3727 ratios. We do not know at this point about the spectra of low luminosity galaxies at high redshifts. It can be nevertheless seen that a given type of spectrum (high [O III] λ 5007/[O II] λ 3727) is found almost exclusively below a luminosity threshold which is low at zero redshift ($M_{B,AB} \sim -18.5$), increases to $M_{B,AB} \sim -20.5$ at $z \sim 0.7$, and has evidently increased to above $M_{B,AB} \sim -23$ at $z \sim 1.4$. One may interpret these basic trends seen in our data within a "downsizing" picture" (Cowie et al. 1996).

"Down-sizing" as originally introduced by Cowie et al. (1996) defined "forming galaxies" as those in which the timescale of formation M_*/SFR was less than the Hubble time at the redshift in question. Cowie et al. (1996) then showed that there existed a threshold in mass below which forming galaxies were found and above which they were not found. "Down-sizing" then referred to the observational fact that this mass threshold decreases (in mass) with cosmic time. This concept has since been generalised to any situation in which signatures of "youthfulness" (e.g. irregular morphologies, blue colours, high equivalent width emission lines, and, as earlier argued in Paper II, low [O/H]) exhibit a similar mass (or more loosely luminosity) threshold which decreases with epoch.

High [O III] λ 5007/[O II] λ 3727 ratios arise from a high ionisation parameter q and/or low metallicities, as shown, e.g., in KD02, their Fig. 1. This is also illustrated in Fig. 6, which shows the oxygen abundance as a function of ionisation parameter for the $0.4 < z < 1.5$ galaxies. It can be seen that the $z \sim 1.4$ galaxies overlap in q and [O/H] the CADIS objects, and avoid the area defined by the more luminous CFRS galaxies with lower q and higher [O/H]. In the next sections, we explore more directly the implied metallicities of the galaxies in our different samples.

4.2. The Pégase2 chemical evolution models

To quantify our results for the chemical evolution of galaxies with cosmic time, we have constructed a grid of chemical evolution models using Pégase2 (Fioc & Rocca-Volmerange 1999). Pégase2 is a user-friendly galaxy evolution code that computes galaxy properties as a function of galaxy age, starting from the properties of simple stellar populations (SSPs), i.e. populations of stars formed simultaneously with the same metallicity. Metallicities between 0.005 and 5 times solar are implemented in the code. The input parameters for Pégase2 are:

(i) $\varphi(M)$, i.e., the shape of the stellar initial mass function (IMF). We adopted a Salpeter IMF, with $\alpha = -2.35$ between 0.1 and 120 $M_{\odot}$.

(ii) Y, i.e., the chemical yields from nucleosynthesis. We used Woosley & Weaver (1995) B-series models for massive stars.

(iii) M_{tot}, i.e., the total mass of gas available to form the galaxy.

(iv) t_{infall}, i.e., the timescale on which the galaxy is assembled. The model assumes that galaxies are built by continuous infall of primordial (zero metallicity) gas with an infall rate that declines exponentially as:

$$\dot{M}(t) = (M_{tot} \cdot e^{-t/t_{infall}})/t_{infall}. \quad (1)$$

The total mass of the galaxy at a given time t is then given by:

$$M(t) = M_{tot} \cdot (1 - e^{-t/t_{infall}}). \quad (2)$$

(v) $\psi(SFR)$, i.e., the functional form of the star formation rate. We adopted a star formation rate of the form:

$$\psi(t) = M_{gas}(t) \cdot p_2 \cdot e^{-t/t_1}/t_1, \quad (3)$$

where $p_2 \cdot e^{-t/t_1}/t_1$ respresents a kind of star formation "efficiency", in the sense that it is $SFR(t)/M_{gas}(t)$. The mass of the gas in the model galaxy at a time t, $M_{gas}(t)$, is equal $M(t) - M_*(t)$, where $M_*(t)$ is the mass locked up into stars at the time t. Models with $t_{infall} > t_1$ are not very likely, since the star formation effectively ceases, even though gas is still infalling. We therefore restricted our grid to models with $t_{infall} \leq t_1$.

(vi) A_V, i.e., the extinction due to dust. The "inclination-averaged" extinction prescription that is implemented in Pégase2 was included in the construction of our models.

To summarize, the set of Pégase2 models we are using consists of the following: it is assumed that there is a reservoir of primordial gas that feeds the "galaxy". The galaxy forms stars with a rate $\psi(t) = (M_{gas}(t) \cdot p_2 \cdot e^{-t/t_1})/t_1$, and we follow the evolution of the model galaxy in the luminosity-metallicity diagram as a function of time. The model galaxy is treated as a single zone with uniform chemical composition and without outflow. This oversimplification is appropriate to get a basic understanding of how fundamental parameters, such as SFR and gas supply, roughly affect galaxy properties such as luminosity and metallicity.

We stress that we do not assign any particular physical significance to these models, but simply use them as means to explore reasonable possibilities. By varying the parameters we can get an understanding of how different evolutionary histories are represented in the [O/H]-M_B plane.

4.3. Constraints on the chemical evolution of galaxies

We constructed a large grid of Pégase2 models to explore which region of the parameter space could reproduce the constraints imposed by the local metallicity-luminosity relation and by the metallicities and luminosities of galaxies at higher redshifts. To build the grid, we varied t_1 (in Gyrs), p_2 (dimensionless), t_{infall} (in Gyrs), and M_{tot} (in solar masses). Fig. 7 shows the relation between the gas abundance 12+log(O/H) versus the absolute B magnitude (in the AB system) for a set of different illustrative models in the grid. In the figure, the symbols along each track indicate the age of the model galaxy, varying from 1 to 13 Gyrs from bottom to top of each track. With reference to the figure the following should be noted:

(i) Models with short t_{infall} and $t_{infall} << t_1$ in Fig. 7 (e.g., $t_{infall} = 1$ and $t_1 = 8$) are models in which the mass of gas in the reservoir of gas is transferred to the galaxy in a short time, after which the gas infall practically stops, resulting in gas rich galaxies at early times. The galaxy subsequently forms stars in a roughly "closed-box"-like scenario.

(ii) Increasing t_{infall} (but still keeping $t_{infall} < t_1$, e.g., $t_{infall} = 4$ and $t_1 = 8$) results in models in which the galaxy reaches a high metallicity at early times. Ultimately, models with $t_1 = t_{infall}$ reach their end metallicity after ~ 1 Gyr, and afterwards their metallicity remains approximately constant while the luminosity decreases. This results in an almost horizontal evolution in the luminosity-metallicity diagram with [O/H] effectively constant over a long period of time.

(iii) Varying M_{tot} results in an horizontal shift of the models as shown in Fig. 7 for two

typical masses ($M_{tot} = 2.5 \times 10^{11} M_{\odot}$, and $M_{tot} = 1.6 \times 10^{10} M_{\odot}$).

Searching for Pégase2 models consistent with the observed metallicities and luminosities of galaxies, we notice a constraint for the models given by the observed properties of local galaxies: the evolution of the model galaxies in the metallicity-luminosity diagram, following the Pégase2 tracks, has to lead to the region occupied by local galaxies today. If galaxies started at very high z they get in the region of the metallicity-luminosity relation today after about 13 Gyrs. But they could get there at younger ages if they started their evolution well after the Big Bang (see below).

The existence of relatively high luminosity galaxies with relatively low metallicities implies that the horizontal "constant-metallicities" models described in (ii) are unlikely. These galaxies would have to fade too much following the horizontal models (ii) to reach the local metallicity-luminosity relation: e.g., in Paper II in Sections 4.1 and 4.2 it was discussed that it is unlikely that CFRS galaxies can fade by more than 2.5 mag to the present epoch.

Thus, a key point seen in Fig. 7 is that galaxies which are observed far from the local luminosity-metallicity relation (i.e., with much lower metallicities) need to have young ages (i.e., be near the start of their evolutionary track) and to follow a "closed-box"-like model (see (i) above) in order to reach the region of the luminosity-metallicity relation of galaxies today, by moving vertically or diagonally and not horizontally, because they need a substantial increase in [O/H].

In the following, we adopt a representative set of Pégase2 models to discuss the chemical evolution of galaxies from $z \sim 1.4$ to today. Specifically, we will use models with fixed $t_1 = 8$ Gyrs and $t_{infall} = 1$ Gyr, and different M_{tot} and p_2. These models are highlighted in Fig. 7 by gray/red lines and filled symbols, and reported in Fig. 8. The selected models have a range of parameters from $M_{tot} = 2.5 \times 10^{11} M_{\odot}$, $p_2 = 1$ (right in Fig. 8), to $M_{tot} = 5.8 \times 10^{9} M_{\odot}$ and $p_2 = 0.3$ (left).

We are not so much interested in precise quantitative arguments, but rather in understanding the qualitative behaviour. Given the global model properties discussed above, the specific choice of models in Figs. 8 and 9 should not affect the general conclusions we draw below.

4.4. Results from the comparison of Pégase2 models and observations

In order to discuss the evolution of the metal abundance of the star forming gas in galaxies from $z = 0$ to $z \sim 1.5$, we compare the Pégase2 models discussed above with the

observed luminosities and metallicities of the five $z \sim 1.4$ galaxies in Fig. 8. Included in the figure are also the intermediate redshift CFRS galaxies, and the location of local KISS and NFGS galaxies listed in Section 2.2.

It is quite noticeable that there is an age-redshift relation along a given Pégase2 track. For example, despite the large scatter, the bright, $M_{B,AB} < -19.5$, $z \sim 1.4$ galaxies (black filled squares) appear to be "younger" than $0.7 < z < 0.9$ galaxies (red filled squares) in the sense that they lie towards the beginning of the luminosity-metallicity track. The latter appear in turn to be on average "younger" than most $0.5 < z < 0.7$ galaxies (green filled squares) which themselves actually overlap significantly on the diagram with the metallicity-luminosity relation traced by nearby galaxies. The tracks of the Pégase2 models suggest that the bright star forming $z \sim 1.4$ galaxies are likely to evolve into the population of less luminous but nonetheless rather massive, metal-rich galaxies that appear in the $0.5 < z < 0.9$ galaxy population. The observation of this age-redshift effect is not surprising, and indeed is reassuring!

Subsequent evolution along the Pégase2 model tracks allows us to speculate about what are specifically the $z = 0$ descendants of the intermediate-z galaxies that we are studying. On the [O/H] vs. $M_{B,AB}$ plane at redshift zero these appear to be massive disk galaxies. The observed I-band HST morphologies of our $z \gtrsim 0.5$ galaxies cover a wide range, with some galaxies having a very compact appearance, and others being extended objects, including regular disks (see Paper II). These morphologies are expected to describe well the distribution of the star forming gas, as they picture the $z \sim 1$ galaxies in approximately the rest-frame B-band, where recent star formation dominates the light emission. We therefore suspect that the metal-enriched reservoirs of star forming gas that we are studying in this paper are being mostly consumed to build up both the disk and the bulge components of spiral galaxies. This interpretation is in agreement with other studies which argue for a substantial build up of stellar mass in disks (see, e.g., Lilly et al. 1998) and bulges (see, e.g., Carollo et al. 1997, 1998; Carollo 1999; Carollo et al. 2001, 2002) at intermediate epochs.

Adding the low luminosity CADIS galaxies from Maier et al. (2004) to the metallicity-luminosity diagram (Fig. 9), we note an interesting fact: the rate of evolution of galaxies along their tracks appears to depend on luminosity (mass). What we mean by this is as follows: At the lookback time of about 6 Gyrs ($z \sim 0.6$) at which a significant fraction of more massive $M_{B,AB} \lesssim -20$ galaxies are still close to the zero redshift metallicity-luminosity relation, the lower luminosity (lower mass) objects at $M_{B,AB} \gtrsim -19$ sampled by CADIS are already quite far from the local metallicity-luminosity. Moreover, the metallicity-luminosity relation of the combined CADIS+CFRS $0.4 < z < 0.7$ sample (green solid line) shows a change in slope compared to the local metallicity-luminosity relation, in the sense that the offset in

metallicity between $z \sim 0$ and $0.4 < z < 0.7$ is larger at lower luminosity than at higher luminosity. This may be due to the fact that lower luminosity (mass) galaxies began their most rapid evolution later than high luminosity (mass) galaxies, as also suggested by the Pégase2 models (see also Kobulnicky et al. 2003). As we look back further in time, we find signs for departures from the $z = 0$ metallicity-luminosity relation occuring at progessively higher luminosities (or masses).

It is important to address possible selection effects in Figs. 8 and 9. In particular, there is no observational reason why the $z \sim 1.4$ galaxies could not have had [O/H] ~ 9 , nor why the most luminous CFRS objects could not have had [O/H] ~ 8.5. As noted earlier, the CADIS sample may be somewhat biased towards lower [O/H] by the [OIII] selection.

To further clarify the effects seen in Fig. 9, one can see that there are (broadly speaking) the signatures of the "downsizing" effect described in Section 4.1 in the sense that: (a) at $z < 0.7$ (green symbols) nearly all galaxies with $M_{B,AB} \lesssim -20$ are fairly close to the low-z [O/H]-M_B relation (there being one obvious exception); (b) at $0.7 < z < 0.9$, this is true only for $M_{B,AB} \lesssim -21.3$; and (c) at $z \sim 1.4$ even the most luminous galaxies are evolved off of the low redshift [O/H]-$M_{B,AB}$ relation.

However, it should be noted that the samples of galaxies at $0.5 < z < 0.9$ and $z \sim 1.4$ and the range in luminosities (particularly for $z > 0.7$) are both quite small and somewhat heterogeneously selected. Therefore, additional measurements of metallicities at $z > 0.5$ of larger samples of galaxies are required to establish a change of the slope of the metalicity-luminosity relation at these redshifts, as indicated by the analysis of the metallicity-luminosity relation of our rather small sample. This could provide more direct evidence for a "downsizing" scenario.

5. Conclusions

The metallicity of the star forming gas has been measured for five galaxies at $z \sim 1.4$ using new near-infrared VLT-ISAAC spectroscopy in the H- and J-band, and already available measurements of the emission line flux of the [O II] λ 3727 line, by which the galaxies were selected. Using the measurements of [O II] λ 3727, Hβ, [O III] λ 5007, Hα, and upper limits for [N II] λ 6584 it was possible to determine the extinction, oxygen abundances, and extinction corrected star forming rates for these luminous ($M_{B,AB} < -21.5$) galaxies. The comparison between Pégase2 chemical evolution models, and the observed properties of galaxies at $z \sim 1.4$, CFRS galaxies at $0.5 < z < 0.9$, lower luminosity CADIS galaxies at $0.4 < z < 0.7$, and more luminous Lyman Break Galaxies (LBGs) at $z \sim 3.1$, lead us to the

following conclusions:

1. The source of gas ionisation in the five $z \sim 1.4$ galaxies for which we measured oxygen abundances is not associated with AGN activity, as derived from the $\log([\mathrm{O\,III}]\,\lambda\,5007/\mathrm{H}\beta)$ versus $\log([\mathrm{N\,II}]\,\lambda\,6584/\mathrm{H}\alpha)$ diagnostic diagram.

2. All the $z \sim 1.4$ galaxies have the high $[\mathrm{O\,III}]\,\lambda\,5007/[\mathrm{O\,II}]\,\lambda\,3727$ and $[\mathrm{O\,III}]\,\lambda\,5007/\mathrm{H}\beta$ line ratios which are typical of the lower luminosity intermediate-z CADIS galaxies (although it should be noted that CADIS is [OIII]-selected and may be slightly biased towards high [OIII]/[OII]) and of the more luminous LBGs at higher z. This is in contrast with the bright, intermediate-z CFRS galaxies, which show low $[\mathrm{O\,III}]\,\lambda\,5007/[\mathrm{O\,II}]\,\lambda\,3727$ and $[\mathrm{O\,III}]\,\lambda\,5007/\mathrm{H}\beta$ ratios. The basic trends in our data are consistent with a "downsizing" picture in the sense that a given type of spectrum (high $[\mathrm{O\,III}]\,\lambda\,5007/[\mathrm{O\,II}]\,\lambda\,3727$) is found almost exclusively below a luminosity threshold which is low at zero redshift ($M_{B,AB} \sim -18.5$), increases to $M_{B,AB} \sim -20.5$ at $z \sim 0.7$, and has evidently increased to above $M_{B,AB} \sim -23$ at $z \sim 1.4$.

3. Analysis of a set of Pégase2 models has shown that galaxies which are observed far from the local luminosity-metallicity relation (i.e., with much lower metallicities) need to have young ages (i.e., be near the start of their evolutionary track) and to follow a roughly "closed-box"-like model to reach the region of the luminosity-metallicity relation of galaxies today.

4. There is an age-redshift relation along a given Pégase2 track. The bright, $M_{B,AB} < -19.5$, $z \sim 1.4$ galaxies appear to be "younger" than $0.7 < z < 0.9$ galaxies, and the latter appear in turn to be on average "younger" than most $0.5 < z < 0.7$ galaxies. The tracks of the Pégase2 models suggest that the bright star forming $z \sim 1.4$ galaxies are likely to evolve into the population of relatively less luminous but nonetheless rather massive, metal-rich galaxies that appear in the $0.5 < z < 0.9$ galaxy population.

5. Interestingly, the rate of evolution of a galaxy along its track appears to depend on luminosity (mass). As we look back in time, we find indications for departures from the local metallicity-luminosity relation occuring at progessively higher luminosities (or masses). This provides further support for a "downsizing" picture of galaxy formation, at least from $z \sim 1.4$ to today.

We would like to thank the anonymous referee for his or her suggestions and comments. C.M. acknowledges support from the Swiss National Science Foundation.

REFERENCES

Carollo, C.M., Stiavelli, M., de Zeeuw, P.T., Mack, J., 1997, AJ 114, 2366

Carollo, C.M., Stiavelli, M., Mack, J., 1998, AJ 116, 68

Carollo, C.M., 1999, ApJ, 523, 566

Carollo, C. M. & Lilly, S. J. 2001, ApJ, 548, 153, Paper I

Carollo, C.M., Stiavelli, M., de Zeeuw, P.T., Seigar, M., Dejonghe, H., 2001, ApJ 546, 2165

Carollo, C.M., Stiavelli, M., Seigar, M., de Zeeuw, P.T., Dejonghe, H., 2002, AJ 123, 159

Chary & Elbaz, 2001, ApJ, 556, 562

Cowie et al., 1995, Nature 377, 603

Cowie, L. L., Songaila, A., Hu, E. M & Cohen, J. G., 1996, AJ, 112, 839

Crampton, D., & Lilly, S.J. 1999, in ASP Conf. Ser. 191, 229

van Dokkum, P.G., Kriek, M., Rodgers, B. et al. 2005, ApJ, 622, 13

Ellison, S.L. & Kewley, L. J., 2005, astro-ph/0508627

Fioc, M. & Rocca-Volmerange, B., 1999, astro-ph/9912179

Grevesse, N., Noels, A., Sauval, A. J. 1996. Standard Abundances, ed. S. S. Holt and G. Sonneborn, Cosmic Abundances: Proc. of the 6th annual October Astrophysics Conference, ASP Conference Ser., 99, 117 (San Francisco: Astron. Soc. of the Pacific)

Hippelein, H., Maier, C., Meisenheimer, K. et al. 2003, A&A, 402, 65

Jansen, R. A., Fabricant, D., Franx, M. et al, 2000, ApJS, 126, 331

Kennicutt, R. C., Jr. 1998, ARA&A, 36, 189

Kewley, L.J., Heisler, C.A., Dopita, M.A.& Lumsden, S. 2001, ApJS, 132, 37

Kewley, L.J. & Dopita, M.A. 2002 ApJSS, 142, 35, KD02

Kobulnicky, H. A. & Koo, D. C. 2000, ApJ, 545, 712

Kobulnicky, H. A., Wilmer C. N. A., Weiner, B. J. et al. 2003, ApJ, 599, 1006

Kobulnicky, H. A. & Kewley, L.J. 2004, ApJ, 617, 240

Le Fevre, O., Crampton, D., Lilly, S. J., Hammer, F., & Tresse, L., 1995, ApJ, 455, 60

Liang, Y. C., Hammer, F., Flores, H. et al. 2004, A&A, 423, 867

Lilly, S. J., Le Fevre, O., Crampton, D., Hammer, F. & Tresse, L. 1995 ApJ, 455, 50

Lilly, S. J., Hammer, F., Le Fevre, O., & Crampton, D., 1995b, ApJ, 455, 75

Lilly, S. J., Le Fevre, O., Hammer, F., & Crampton, D. 1996, ApJ, 460, 1

Lilly, S. J., Schade, D., Ellis, R. et al., 1998, ApJ, 500, 75

Lilly, S.J, Carollo, C.M. & Stockton, A. 2003, ApJ, 597, 730, Paper II

Madau, P., Ferguson, H. C., Dickinson, M. E., et al., 1996, MNRAS, 283, 1388

Maier, C., 2002, PhD Thesis, Naturwissenschaftlich-Mathematische Gesamtfakultät der Universität Heidelberg, Germany

Maier, C., Meisenheimer, K., Thommes, E. et al. 2003, A&A, 402, 79

Maier, C., Meisenheimer, K., Hippelein, H., 2004, A&A, 418, 475

Maier, C., Lilly, S., Carollo, C. M., Stockton, A. & Brodwin. M., 2005, ApJ, 634, 849, Paper III

Maier, C., Lilly, S., Carollo, C. M., Stockton, A. & Brodwin. M., 2005, ApJ in press, astro-ph/0508239, Paper III

Melbourne, J. & Salzer, J. J. 2002, AJ, 123, 2302

Pagel, B. E. J., Edmunds, M. G., Blackwell, D. E. et al. 1979, MNRAS, 189, 95

Perez-Gonzalez, P. G., Rieke, G. H., Egami, E. et al., 2005, astro-ph/0505101

Pettini, M., Shapley, A. E., Steidel, C. C. 2001, AJ, 554, 981

Pettini, M., Rix, S.A., Steidel, C.C. et al. 2002, Ap&SS, 281, 461

Salzer, J. J., Lee, J.C., Melbourne, J. et al., 2005, ApJ, 624, 661

Shapley, A., Erb, D. K., Pettini, M. et al. 2004, ApJ, 612, 108

Somerville, R.S., Lemson, G., Sigad, Y. et al. 2001, MNRAS, 320, 504

Tran, K. H., Lilly, S.J., Crampton, D. and Brodwin, M. , 2004, ApJ, 612, 89

Woosley, S. E. & Weaver, T. A. 1995, ApJS, 101, 181

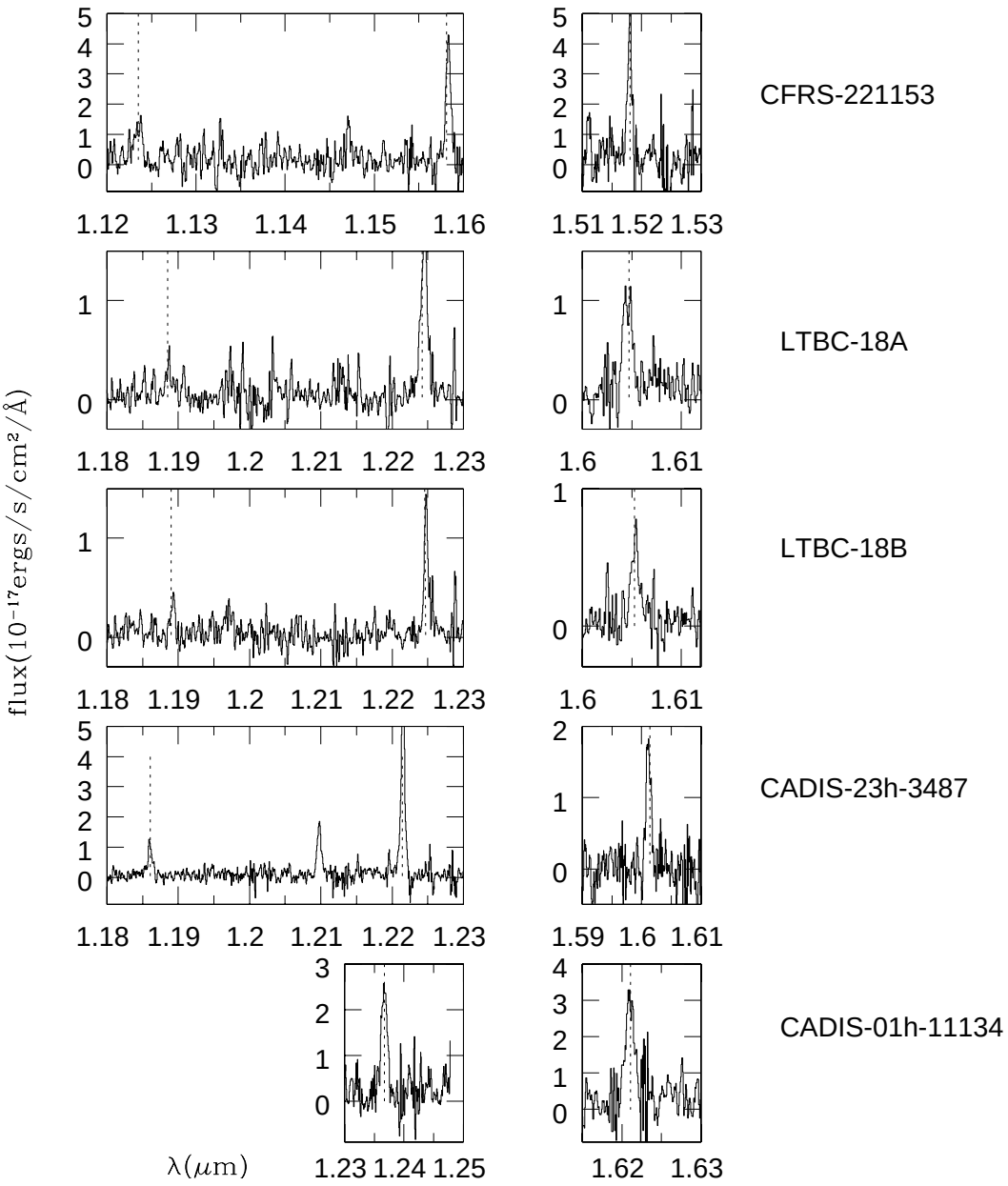

Fig. 1.— The near-infrared spectra of the five $z \sim 1.4$ galaxies showing Hβ and [O III] λ 5007 from J-band spectra (left panel), and Hα from H-band spectra (right panel). The location of the respective emission line is shown by vertical dashed lines. Note that the Hβ line of CADIS-01h-11134 coincides with a strong OH sky line, so the respective flux could not be measured.

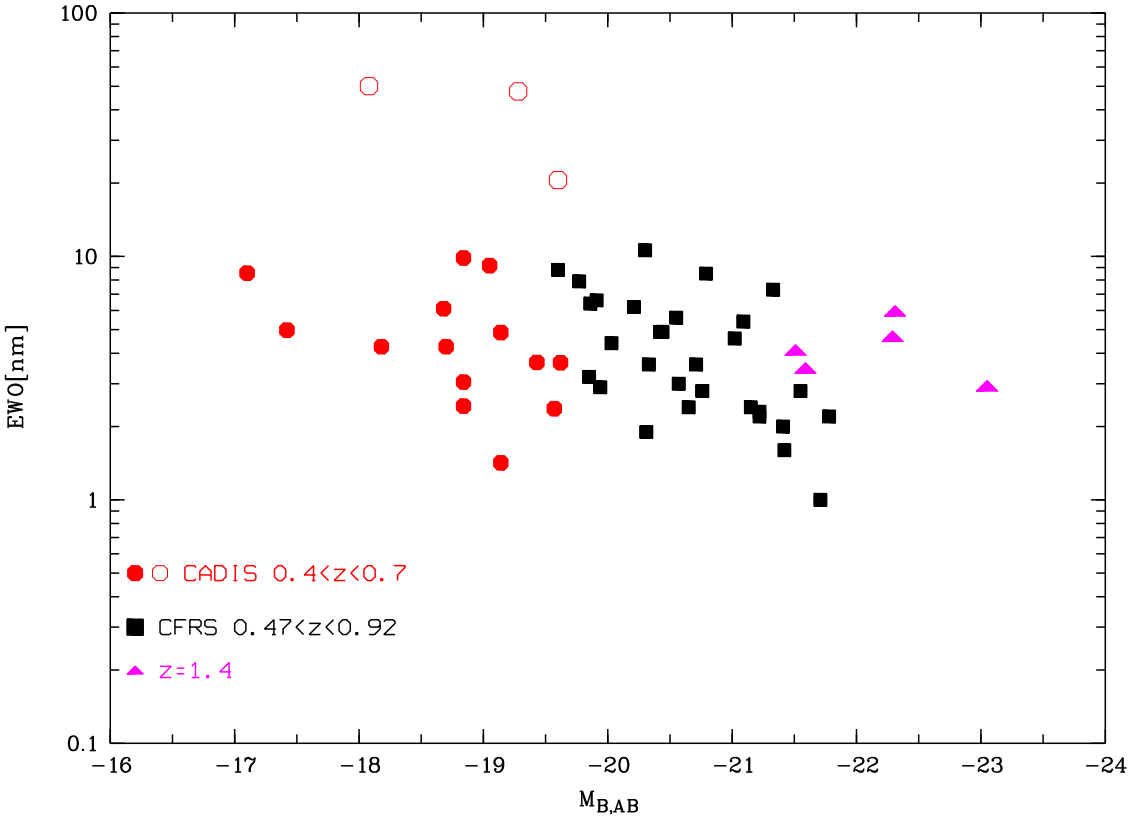

Fig. 2.— Line equivalent widths (EWs) at rest wavelength versus absolute blue magnitude for the $0.4 < z < 0.7$ CADIS galaxies and $0.47 < z < 0.92$ CFRS galaxies in our comparison samples, and for the $z \sim 1.4$ galaxies. The distribution of the EWs of CADIS objects is consistent with the EW distribution of the CFRS sample and $z \sim 1.4$ galaxies, except three CADIS objects at $z \sim 0.4$ with particular high equivalent widths (open circles), which are excluded from the comparison sample for the further discussion.

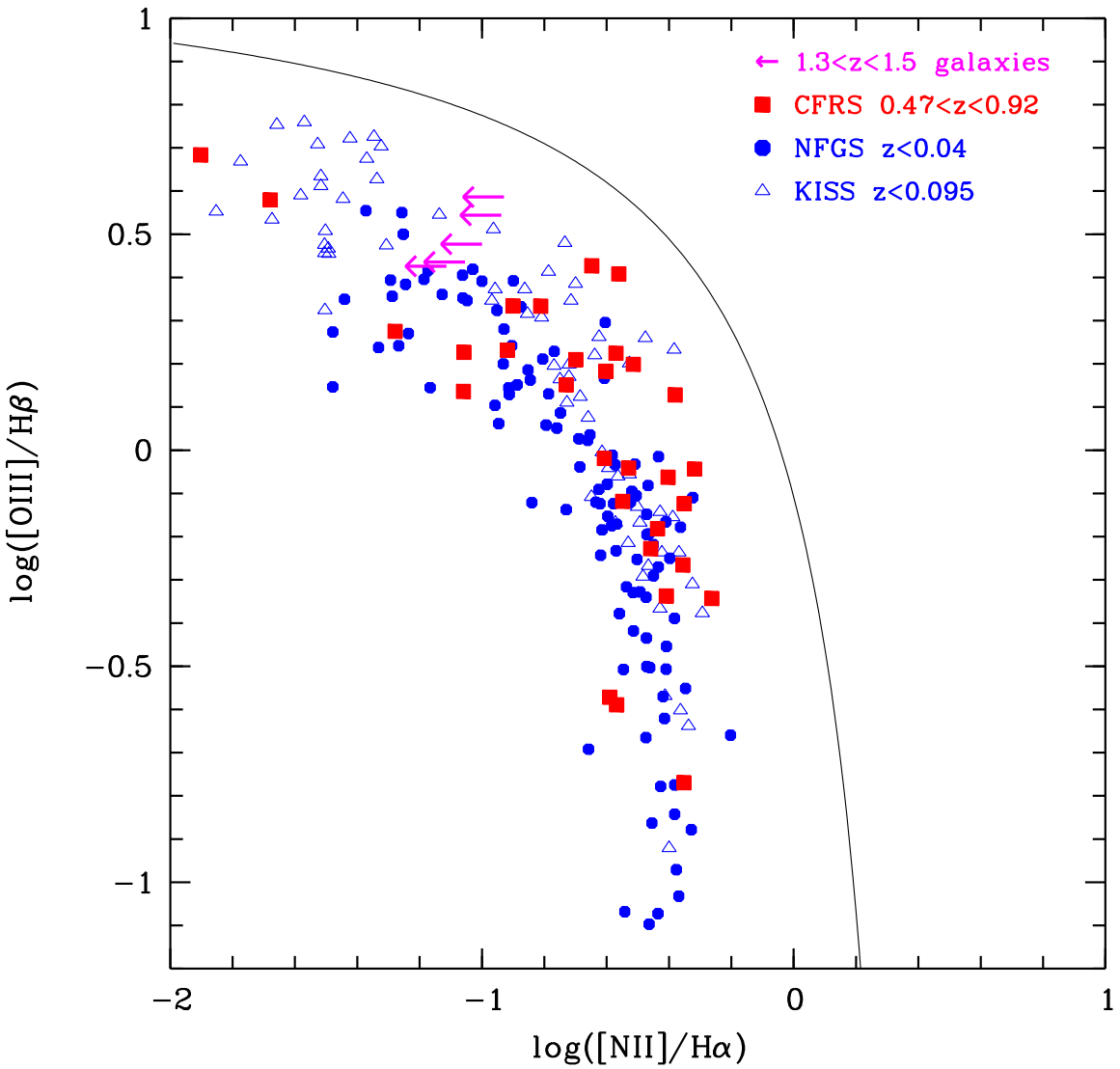

Fig. 3.— Diagnostic diagram to disentangle star-formation dominated galaxies from AGNs. The position of the five galaxies at $z \sim 1.4$ is shown by the arrows, since only upper limits for [N II] λ6584 could be derived. Also plotted are the 30 $0.47 < z < 0.92$ CFRS galaxies of Paper III (filled squares), 108 local NFGS galaxies from Jansen et al. (2000, filled circles), and 70 local KISS galaxies from Melbourne & Salzer (2002, open triangles). All the plotted galaxies, including the $z \sim 1.4$ galaxies, lie below the solid line, i.e., the theoretical threshold computed by Kewley et al. (2001) above and to the right of which galaxies are dominated by an AGN. In all plotted galaxies the emission is thus dominated by star formation.

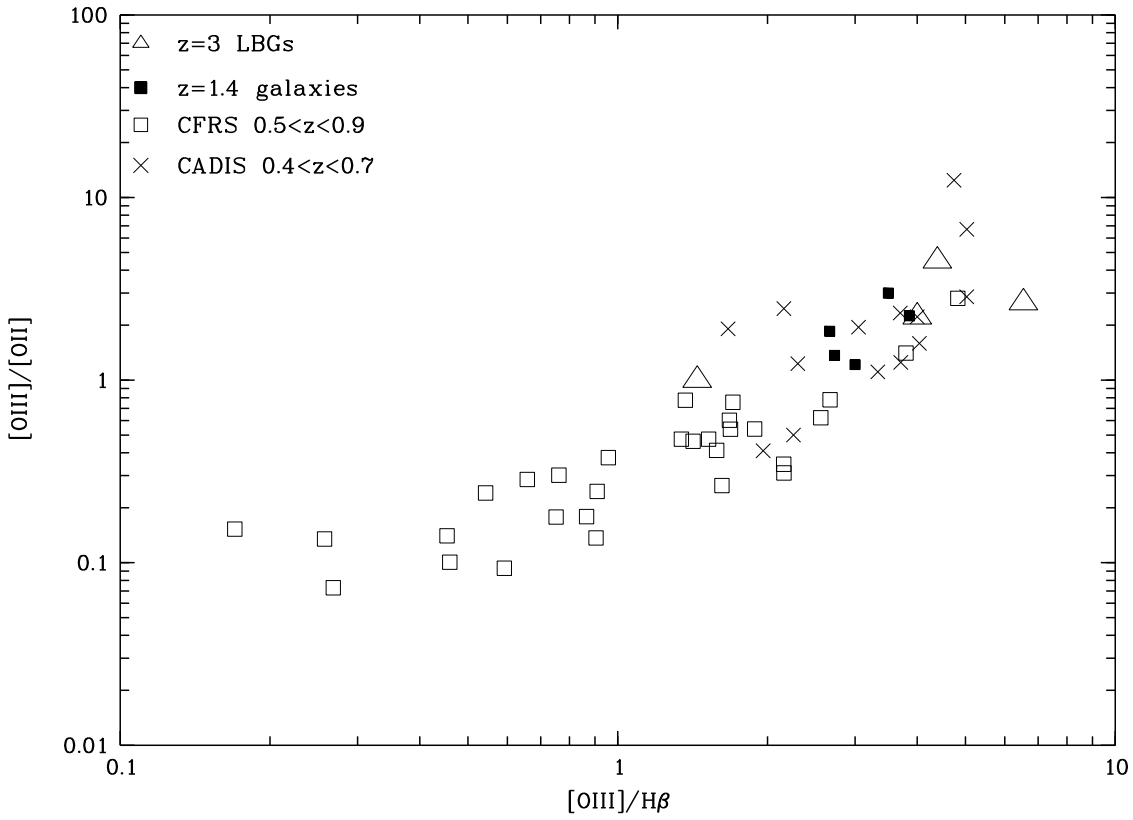

Fig. 4.— Line ratios [O III] λ 5007/[O II] λ 3727 vs. [O III] λ 5007/Hβ for the $z \sim 1.4$ galaxies (solid squares). Also plotted are the 30 $0.47 < z < 0.92$ bright CFRS galaxies (open squares), the $0.4 < z < 0.7$ CADIS galaxies of Maier et al. (2004, crosses), and the $z \sim 3$ LBGs galaxies (open triangles). The five $z \sim 1.4$ galaxies have the high [O III] λ 5007/[O II] λ 3727 ratios that are typical of the lower luminosity CADIS galaxies and of the more luminous higher-z LBGs.

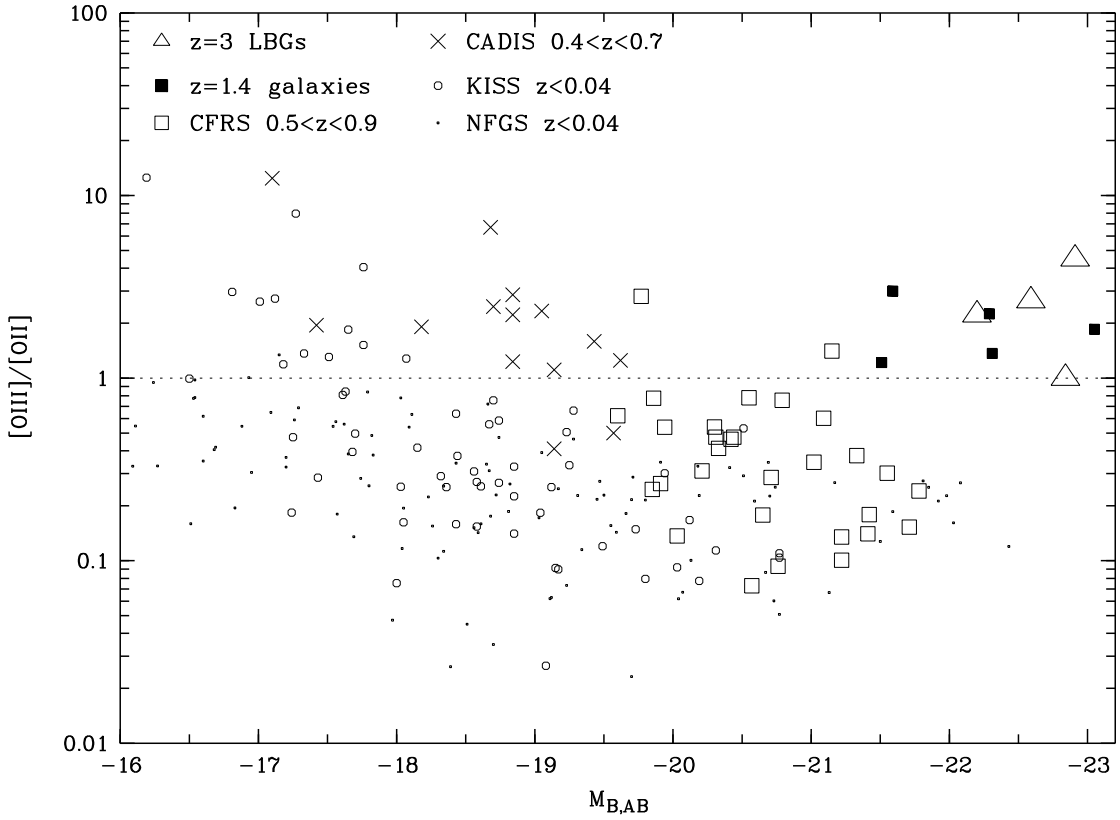

Fig. 5.— [O III] λ 5007/[O II] λ 3727 vs. $M_{B,AB}$ for galaxies at $0 < z < 1.5$ with symbols as in Fig. 4, with additional plotted local KISS (open circles) and NFGS (dots) galaxies. The basic trends in our data are consistent with a "downsizing" picture (Cowie et al. 1996) in the sense that a given type of spectrum (high [O III] λ 5007/[O II] λ 3727) are found almost exclusively below a luminosity threshold which is low at zero redshift ($M_{B,AB} \sim -18.5$), increases to $M_{B,AB} \sim -20.5$ at $z \sim 0.7$, and has evidently increased to above $M_{B,AB} \sim -23$ at $z \sim 1.4$.

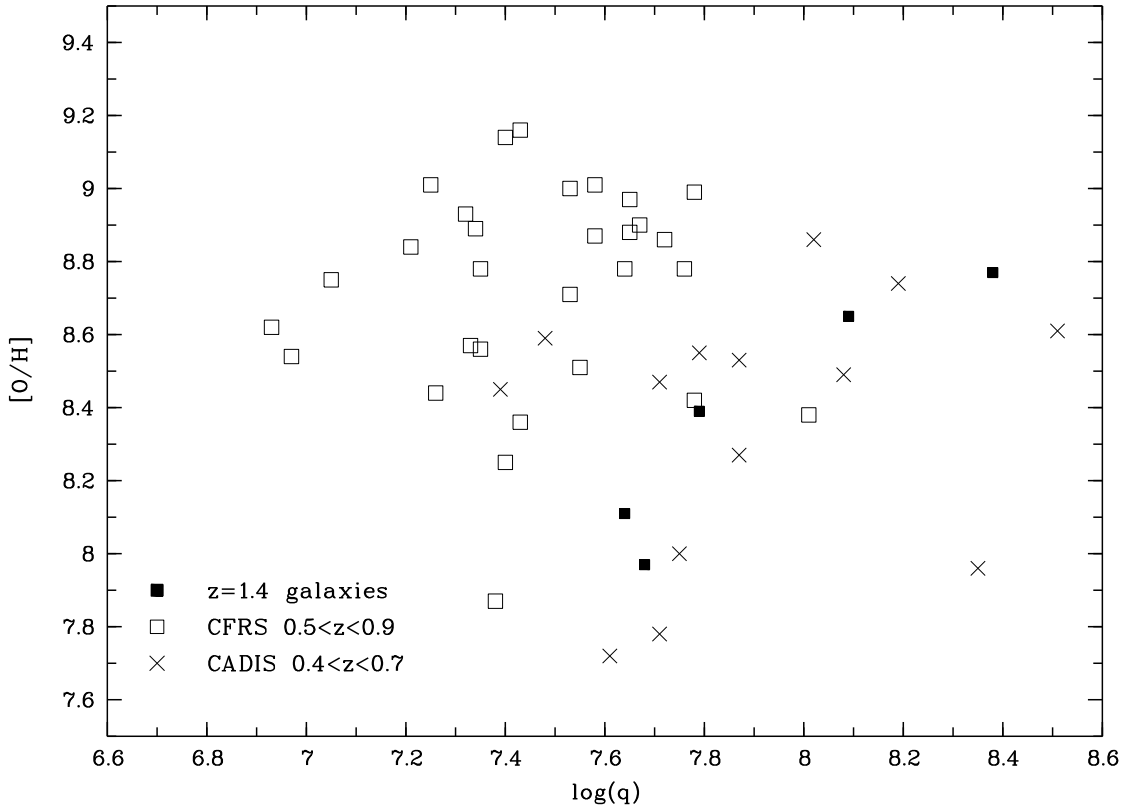

Fig. 6.— Oxygen abundance vs. ionisation parameter for galaxies at $0 < z < 1.5$ with symbols as in Fig. 4. The $z \sim 1.4$ galaxies overlap in q and [O/H] the CADIS objects, and avoid the area defined by the more luminous CFRS galaxies with lower q and higher [O/H], showing that the high [O III] λ 5007/[O II] λ 3727 ratios shown in Fig. 5 arise from either or both high ionisation parameter q and low metallicities.

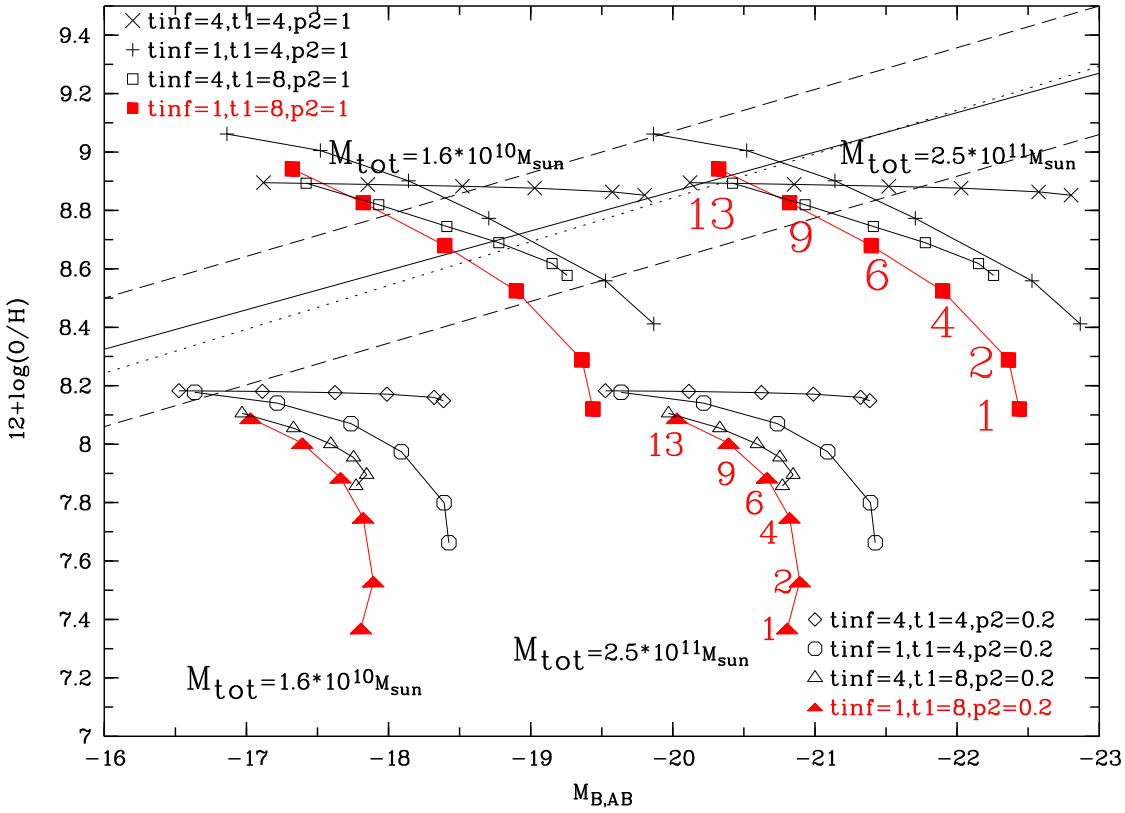

Fig. 7.— Several Pégase2 models for different t_1, p_2, t_{infall}, and M_{tot}, compared to the local metallicity-luminosity relation. The nearby NFGS and KISS galaxies have oxygen abundances lying between the dashed lines (with the solid and dotted lines indicating the mean local relation for NFGS and KISS galaxies, respectively).

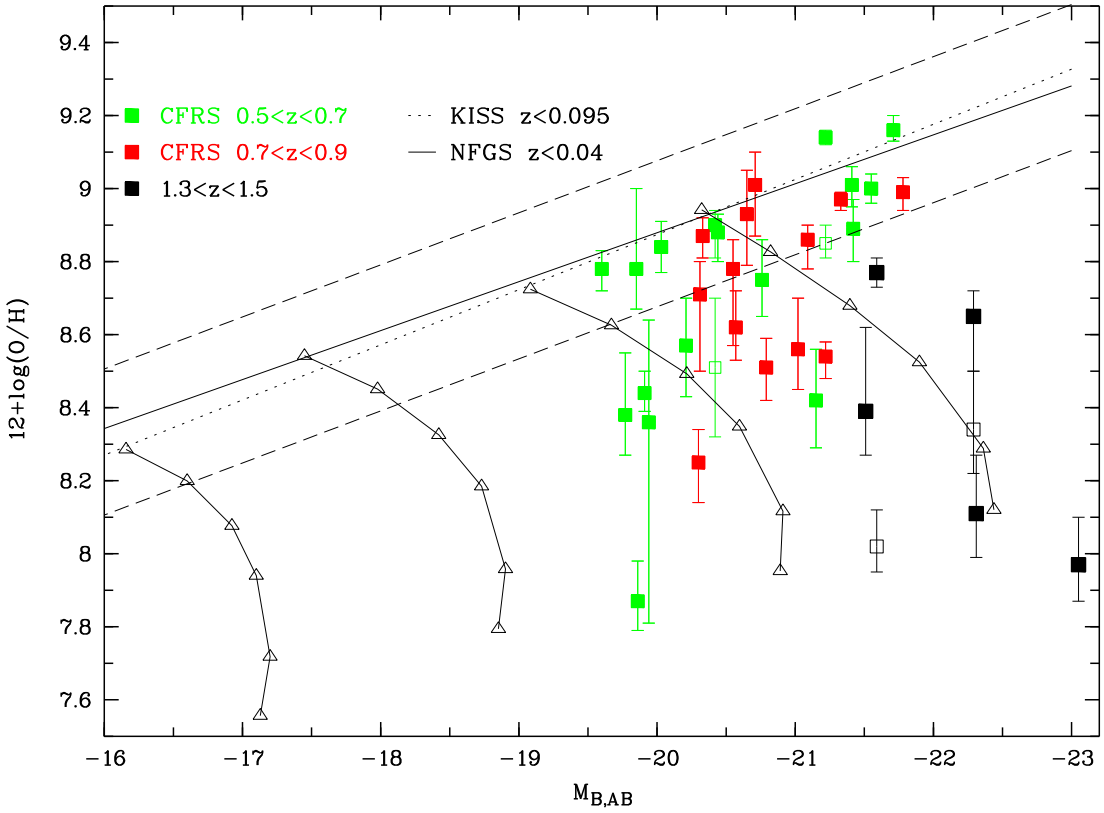

Fig. 8.— Oxygen abundance vs. $M_{B,AB}$ for the $z \sim 1.4$ galaxies of our sample (black filled squares). Plotted are also the CFRS galaxies, split in two redshift bins: CFRS galaxies at $0.5 < z < 0.7$ are plotted as green filled squares, while CFRS galaxies at $0.7 < z < 0.9$ are plotted as red filled squares. Open squares are the alternative (but less probable) oxygen abundance solutions, as discussed in Section 3.3 and Fig. 4 of Paper III. The nearby NFGS and KISS galaxies have [O/H] lying between the dashed lines (with the solid and dotted lines indicating the mean local relation for NFGS and KISS galaxies, respectively). All oxygen abundances were uniformly measured using the code based on KD02 models. The tracks show a subset of theoretical Pégase2 models which are consistent with the local metallicity-luminosity relation (see text).

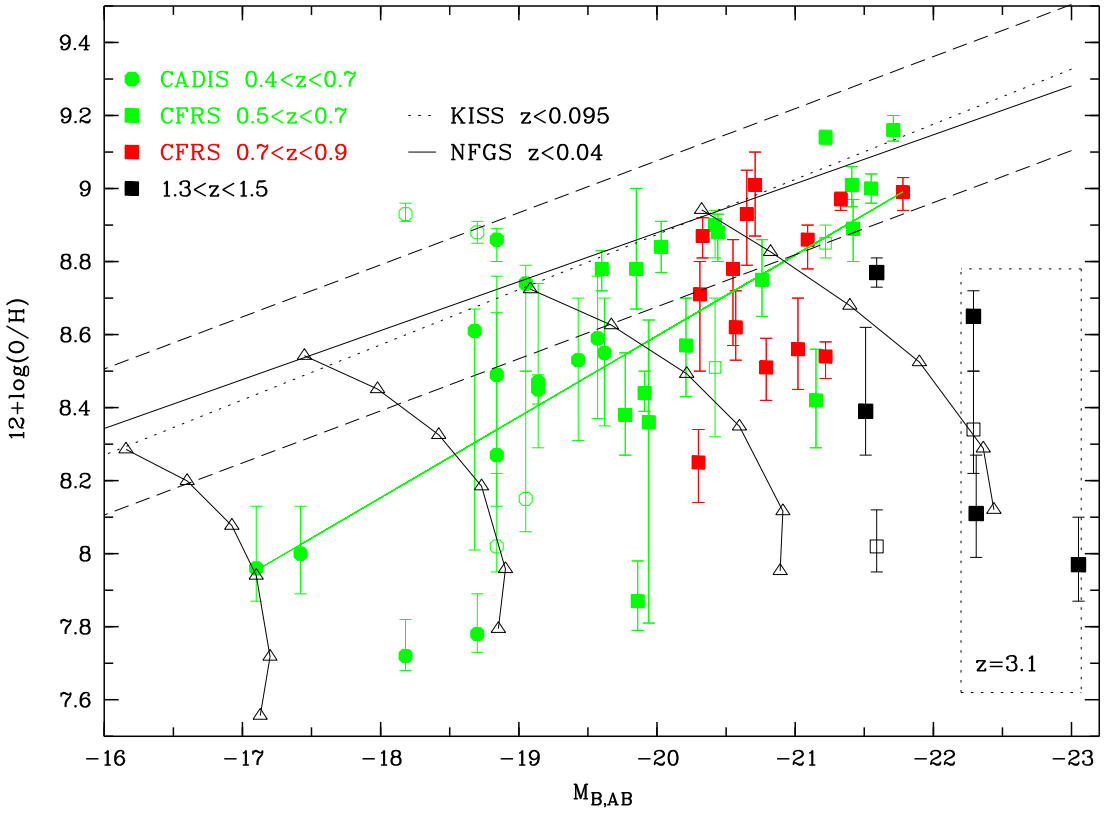

Fig. 9.— Same as Fig. 8, but with additional plotted lower luminosity CADIS galaxies (green filled circles), and LBGs galaxies at $z \sim 3.1$. The location of bright galaxies at $z \sim 3.1$ is shown as a box encompassing the range of $M_{B,AB}$ and [O/H] (without breaking the R_{23} degeneracy) derived for these objects from Fig. 7 in Pettini et al. (2001), which takes also into account the metallicities derived by Kobulnicky & Koo (2000) for $z \sim 3.1$ objects. Open squares and circles are alternative (but less probable) oxygen abundance solutions for some galaxies, as discussed in Section 3.3 and Fig. 4 of Paper III.

Table 1: VLT-ISAAC spectroscopic observations of the five $z \sim 1.4$ galaxies

#	Filter	t_{exp}(s)	Night	Seeing	Telluric Standard[a]
CFRS-221153	H	1200	Oct 03/04 2004	1″.0	Hip101505
CFRS-221153	H	1200	Oct 06/07 2004	1″.0	Hip100881
CFRS-221153	J	3600	Oct 04/05 2004	0″.8	Hip094653
CFRS-221153	J	5400	Oct 06/07 2004	1″.2	Hip100881
LTBC-18A	H	1800	Oct 05/06 2004	1″.2	Hip000183
LTBC-18A	J	5400	Oct 05/06 2004	1″.2	Hip000183
LTBC-18B	H	2000	Oct 03/04 2004	1″.3	Hip109332
LTBC-18B	H	1800	Oct 05/06 2004	1″.2	Hip000183
LTBC-18B	J	6000	Oct 03/04 2004	1″.4	Hip109332
LTBC-18B	J	5400	Oct 05/06 2004	1″.2	Hip000183
CADIS-23h-3487	H	1800	Oct 06/07 2004	1″.0	Hip100881
CADIS-23h-3487	J	5400	Oct 06/07 2004	1″.0	Hip100881
CADIS-01h-11134	H	1200	Oct 08/09 2004	0″.9	Hip108975
CADIS-01h-11134	J	1200	Oct 08/09 2004	0″.9	Hip108975

[a] "Hip" denotes the Hipparcos catalogue from which the telluric standards were selected.

Table 2. Observed and derived quantities for the five $z \sim 1.4$ galaxies

Nr	RA	DEC	$M_{B,AB}$	z	[OII][a]	Hβ[a]	[OIII][a]	Hα[a]	[NII][a,b]	A_V	SFR	[O/H]
CFRS-221153	22 17 40.60	+00 18 21.82	-22.31	1.313	20±2.0	11±1.0	30±3.0	34±3.0	< 3	$0.26^{+0.41}_{-0.26}$	$33.04^{+15.68}_{-8.35}$	$8.11^{+0.16}_{-0.12}$
LTBC-18A	22 17 40.29	+00 20 20.60	-21.59	1.445	4.3±0.4	4±0.8	14±1.4	13±1.2	< 1.5	$0.23^{+0.53}_{-0.23}$	$15.67^{+9.51}_{-3.71}$	$(8.77)^{+0.04}_{-0.10}$[d]
LTBC-18B	22 17 40.15	+00 20 19.10	-21.51	1.446	7.4±0.7	3±0.6	9 ±0.9	7 ±0.7	< 0.7	$0.00^{+0.12}_{-0.00}$	$7.17^{+1.42}_{-0.72}$	$8.39^{+0.23}_{-0.12}$
CADIS-23h-3487	23 15 28.63	+11 23 13.54	-22.29	1.440	12±1.2	7±0.7	27±2.5	17±1.5	< 2	$0.00^{+0.16}_{-0.00}$	$17.23^{+4.02}_{-1.72}$	$(8.65)^{+0.07}_{-0.15}$[d]
CADIS-01h-11134	01 47 33.37	+02 22 12.90	-23.05	1.470	15±1.5	(14±1.4)[c]	32±3.2	39±3.5	< 3	$0.39^{+0.43}_{-0.39}$[c]	$54.98^{+27.27}_{-17.54}$[c]	$7.97^{+0.13}_{-0.10}$[c]

[a]Fluxes are given in 10^{-17}ergs s^{-1}cm^{-2}

[b]For [N II] λ6584 2σ upper limits for the emission line flux are given

[c]Hβ of this object coincides with a strong OH sky line, so the respective flux could not be measured. However, we derived the Hβ flux for this galaxy assuming $A_V = 0.5$ and case B recombination, as discussed in the text.

[d]Alternative (but less probable) oxygen abundances found using the method described in Section 3.3 and Fig. 4 of Paper III are [O/H]=$8.02^{+0.10}_{-0.07}$ for object LTBC-18A, and [O/H]=$8.34^{+0.16}_{-0.12}$ for object CADIS-23h-3487.